

## **Control of surface functional groups on pertechnetate sorption on activated carbon**

Yifeng Wang<sup>1</sup>, Huizhen Gao<sup>1</sup>, Rakesh Yeredla<sup>2</sup>, Huifang Xu<sup>2</sup>, Mike Abrecht<sup>3</sup>, and Gelsomina De Stasio<sup>3</sup>

<sup>1</sup>Sandia National Laboratories, P. O. Box 5800, Albuquerque, New Mexico 87185, USA;

<sup>2</sup>Department of Geology and Geophysics, University of Wisconsin, Madison, Wisconsin 53706; and <sup>3</sup>Synchrotron Radiation Center, University of Wisconsin, 3731 Schneider Dr.

Stoughton, Wisconsin 53589

---

### **Abstract**

<sup>99</sup>Tc is highly soluble and poorly adsorbed by natural materials under oxidizing conditions, thus being of particular concern for radioactive waste disposal. Activated carbon can potentially be used as an adsorbent for removing Tc from aqueous solutions. We have tested six commercial activated carbon materials for their capabilities for sorption of pertechnetate (TcO<sub>4</sub><sup>-</sup>). The tested materials can be grouped into two distinct types: Type I materials have high sorption capabilities with the distribution coefficients (K<sub>d</sub>) varying from 9.5x10<sup>5</sup> to 3.2x10<sup>3</sup> mL/g as the pH changes from 4.5 to 9.5, whereas type II materials have relatively low sorption capabilities with K<sub>d</sub> remaining more or less constant (1.1x10<sup>3</sup> - 1.8x10<sup>3</sup> mL/g) over a similar pH range. The difference in sorption behavior between the two types of materials is attributed to the distribution of surface functional groups. The predominant surface groups are identified to be carboxylic and phenolic groups. The carboxylic group can be further divided into three subgroups A, B, and C in the order of increasing acidity. The high sorption capabilities of type I materials are found to be caused by the presence of a large fraction of carboxylic subgroups A and B, while the low sorption capabilities of type II materials are due to the exclusive presence of phenolic and carboxylic subgroup C. Therefore, the performance of activated

carbon for removing  $\text{TcO}_4^-$  can be improved by enhancing the formation of carboxylic subgroups A and B during material processing.

*Keywords:* Activated carbon; Carbonaceous material; Technetium; Pertechnetate; Surface functional group; Mesoporous material; Adsorption; Oxyanion

---

## 1. Introduction

$^{99}\text{Tc}$  is a fission product with a long half life of  $2.13 \times 10^5$  years [1]. The fate of this radionuclide released from spent fuel alteration is of particular concern in the performance assessment of a high-level waste repository [2]. The behavior of Tc in a geologic environment highly depends on its oxidation state [3]. In a reducing environment, Tc is present in the +IV state, forming sparingly hydroxides  $\text{TcO}_2 \cdot n\text{H}_2\text{O}$ , while, under an oxidizing condition, the predominant form of Tc is pertechnetate ( $\text{TcO}_4^-$ ), which is highly soluble and poorly sorbed by natural materials [4]. Various synthetic or engineered natural materials have been investigated for their potential use for long-term immobilization of  $\text{TcO}_4^-$  in oxic subsurface environments [5, 6]. Among others, activated carbon has been shown to have a relatively high efficiency for retaining  $\text{TcO}_4^-$  [1].

Activated carbon is made from a raw material such as wood, lignite, peat, or coal, typically through a two-stage process: carbonization and activation [7, 8]. In the first stage, the raw material is carbonized at a moderate temperature (200 – 400 °C) in air (for L-carbon) or at a higher temperature (up to 1200 °C) in an inert atmosphere (for H-carbon). In the second stage, the resulting chars are subjected to a partial gasification at a temperature up to 900 °C with  $\text{H}_2\text{O}$  steam or  $\text{CO}_2$ . Due to its high specific surface area, nanoporous structure, and variable surface functional groups, activated carbon is widely used as an adsorbent for removing toxic metals [9-11], oxyanions [12-15], and organic compounds [16-19]. Activated carbon is also used in catalysis [20], electrochemistry [21-22], and hydrogen storage [23].

Several studies have been performed to determine the capability of activated carbon for sorption of  $\text{TcO}_4^-$ . Ito and Yachidate investigated  $\text{TcO}_4^-$  sorption on five activated carbon materials from different sources [24]. They found that activated carbon derived from coconut shell or oil pitch would appear to be most suitable for adsorbing Tc from high level liquid waste while those derived from coal could excel others for its stable performance less affected by other anions. Gu et al. studied the sorption of  $\text{TcO}_4^-$  on activated carbon in various electrolyte solutions [1]. The distribution coefficient ( $K_d$ ) of  $\text{TcO}_4^-$  between solid and liquid was determined to range from  $2.1 \times 10^3$  to  $2.7 \times 10^4$  mL/g. A much higher  $K_d$  ( $\sim 10^6$  mL/g) value was reported for  $\text{TcO}_4^-$  sorption in deionized water [25]. The mechanism for  $\text{TcO}_4^-$  sorption on activated carbon is still unclear. Given the large variability in measured  $K_d$  values, a mechanistic understanding of the sorption process is crucial for selecting or engineering a carbonaceous material for a specific application. In this paper, we systematically test six commercial activated carbon materials for their capabilities for removing  $\text{TcO}_4^-$  and correlate the measured sorption capabilities to the distribution of surface functional groups revealed by acid-base titration and spectroscopic analyses.

## **2. Experimental**

### **2.1. Materials**

Six activated carbon materials used in this study were generously provided by NORIT Americas Inc.: (1) INSUL - a fine ground material with a high pore volume and low density and excellent for insulation, (2) MRX - A special grade of granular material that has been used as a catalyst support in oil refineries, (3) HYDRO-B - a powdered material produced by steam activation of lignite coal under carefully controlled conditions and used for adsorption of organics that cause taste and odor problems in water supplies, (4) HYDRO-4000 – a granular material designed for removing dissolved organics in water treatments and produced by high temperature steam activation of lignite coal, (5) S-51HF – an acid washed powdered activated carbon produced by steam activation of lignite coal and used for a wide range of purification processes, and (6) 12X20DC - another acid washed granular material produced by steam activation of lignite coal and specifically manufactured for cartridge dry cleaning applications. The

powdered materials were crushed derived from the same granular materials (personal communication with Bill Naylor of NORIT America Inc., 2006). The surface areas and pore sizes of these materials were measured with a N<sub>2</sub> BET method [26], using Micromeritics Gemini 2360 surface analyzer.

## 2.2. FTIR and XPEEM

Both Fourier transform infrared spectroscopy (FTIR) and X-ray photoelectron emission spectromicroscopy (XPEEM) were used to identify possible functional groups present on the surface of activated carbon. In the FTIR analysis, the KBr pellets containing about 0.1% activated carbon were prepared by hydraulic press. The spectra were collected from 4000 to 400 cm<sup>-1</sup> on an IR spectrometer. In the XPEEM analysis, the sample was illuminated by a monochromatic X-ray beam that was moderately focused on tens of micrometers, so that it matched the maximum field of view. The sample was held at -20 kV and illuminated at grazing incidence (16°) by X-rays from the synchrotron beamline. The XPEEM electron signal originated close to the sample surface. The magnified photoelectron image was focused onto two microchannel plates and converted into a visible image by a phosphor screen. The image was collected by a slow scan 12 bit digital camera and transferred to a computer using custom acquisition software.

## 2.3. Acid-base titrations

The acid-base titrations were conducted for four representative activated carbons using a Mettler DL25 Autotitrator. The titrations were performed in three electrolyte solutions: de-ionized (D.I.) water, 0.01 M NaCl, and 0.1 M NaCl. In each titration, 0.1 – 0.2 gram of activated carbon was added to 50 mL of electrolyte solution and then titrated with 0.099 M NaOH. Prior to each titration, 0.2 mL 0.093 M HCl solution was added to the sample to make the titration start from an acid pH point. The titration time interval was set to 90 seconds (the maximum time allowed by the instrument) to minimize the possible effect of slow diffusion of ions in nanopores in activated carbon. All titrations were performed under CO<sub>2</sub>-free conditions.

## 2.4. Sorption experiments

All six activated carbon materials were tested for their adsorption capabilities for pertechnetate ( $\text{TcO}_4^-$ ). In each test,  $\sim 0.1$  g of activated carbon was weighed into a 40-mL centrifuge tube and equilibrated with 20 mL de-ionized water overnight. 0.1 mL of  $\text{TcO}_4^-$  ( $10^{-4}$  M) was then spiked into each centrifuge tube. The tubes were shaken for 24 hours. The samples were then centrifuged at 3500 rpm for 5 min. 1 mL of the supernatant of each sample was placed into a vial containing 15 mL cocktail solution. The solution was well mixed and subjected to a liquid scintillation count. The equilibrium pH for sorption was measured at the end of each experiment. Liquid scintillation counts were performed on Tri-CARB Liquid Scintillation Analyzer (Model Standard 2700TR) equipped with the patented time-resolved liquid scintillation counting technique and able to perform a three-dimensional analysis (counts/channel, pulse height in keV, and time) during collecting counts from a sample. Each analysis was performed at a count time of 10 minutes per sample on a channel-by-channel basis. The  $\beta$ -activity was recorded and then converted to a mass concentration. A distribution coefficient ( $K_d$ ) of Tc between the solid and the liquid was calculated from two replicates of measurements.

## 3. Results and discussion

### 3.1 $\text{TcO}_4^-$ sorption on activated carbon

The sorption capability of each activated carbon material was measured as a function of solution pH. The distribution coefficient ( $K_d$ ) is calculated by [6]:

$$K_d = \frac{\text{amount of Tc sorbed on solid/mass of solid}}{\text{amount of Tc dissolved/volume of solution}} \quad (\text{mL/g}). \quad (1)$$

The results are shown in Figure 1. Interestingly, the  $K_d$  values of all six materials we tested fall basically on two separate sorption lines, based on which the materials can be grouped into two types with very distinct sorption behaviors. The distribution coefficients ( $K_d$ ) of type I materials (INSULT, 51HF, and HYDRO-B) show strongly dependent on the pH of solution and vary from  $9.5 \times 10^5$  to  $3.2 \times 10^3$  mL/g as the pH changes from 4.5 to 9.5., whereas the  $K_d$  values of type II materials (MRX, HYDRO-4000, and 12X20DC) remain more or less constant ( $1.1 \times 10^3$  -  $1.8 \times 10^3$  mL/g) over a similar pH range. The

difference in  $K_d$  between the two types of materials could be as large as three orders of magnitude (Figure 1). A mechanistic understanding of the underlying cause for such distinct sorption behaviors between the two types of materials is therefore crucial for selecting or engineering activated carbon for a specific application as an ion adsorbent.

Apparently, this difference cannot be attributed to the variation in specific surface areas or pore structures of the materials, since BET measurements indicate that all six materials have similar specific surface areas and pore sizes (Table 1). The surface area of these materials ranges from 478 to 750  $\text{m}^2/\text{g}$ , with the highest value actually corresponding to a material (HYDRO-4000) with a relatively low sorption capability. Similarly, the pore size of the materials only slightly varies from 4.1 to 5.4 nm.

Surface functional groups are known to have a great influence on the sorption behavior of activated carbon, as observed for other adsorbates such as heavy metals [9, 11, 27, 28] and organic compounds [19, 29]. Figure 1 implies (1) the presence of two major surface functional groups with very different sorption capabilities and (2) the distinct distributions of these functional groups on the two types of materials. Note that the distribution coefficient ( $K_d$ ) can be split into two terms, i.e.,  $\log K_d = \log K'_d + \log N$ , where  $K'_d$  is the complexation constant of a functional group and  $N$  is the population of this functional group on each material. For a functional group with a high complexation constant, the first term would dominate the second term as long as the population of the functional group varies only moderately among different materials. This is why different materials from the same type fall roughly onto a single sorption line in Figure 1, even though a certain degree of variation may exist in the population of functional groups among these materials. Thus, the slope of each line in Figure 1 is mainly determined by the stoichiometry of  $\text{H}^+$  or  $\text{OH}^-$  in the corresponding sorption reaction. Figure 1 also implies that type II materials must be dominated by functional groups all with low sorption capabilities.

### 3.2 Surface functional groups

Various functional groups can form on the surface of activated carbon during activation. Predominant surface functional groups were suggested to include carboxyl, phenolic hydroxyl, carbonyl (quinine type), carboxylic acids, anhydrides, lactone, and cyclic peroxides [30]. In order to identify surface functional groups responsible for  $\text{TcO}_4^-$  sorption, both FTIR and XPEEM analyses were performed on four representative materials (INSUL, S-51HF, HYDRO-4000, and 12X20DC). The obtained FTIR spectra are shown in Figure 2. The assignment of FTIR bands to specific chemical bonds is given in Table 2. The data clearly show the presence of both carboxylic and phenolic groups, although relative proportions of these groups on individual samples are difficult to determine due to the qualitative nature of FTIR measurements [31].

The XPEEM spectra for the same materials are shown in Figure 3. The carbon spectra shows a relatively sharp peak at 286.6 eV and a broad peak near 295 eV for all four samples (Figure 3A), which respectively arise from  $\pi^*$  and  $\sigma^*$  resonances [32, 33]. Sample S-51HF has a peak near 289.3 eV, while sample INSUL has a peak at 291.8 eV, respectively corresponding to  $\text{C-H}^*$  and  $\text{C-O}^*$  resonances [32, 33]. The observed  $\text{C-O}^*$  resonance indicates the significant presence of oxygen-containing functional groups in activated carbon samples, consistent with the FTIR analysis. Note that the carbon spectra alone do not allow us to differentiate the two distinct types of activated carbons in terms of their surface structure difference. This is because the signals from the bulk structure likely mask the carbon spectra from actual surface functional groups, even though the XPEEM analysis itself is limited only within top nanometers beneath the material surface.

The oxygen spectra are expected to be more sensitive than the carbon spectra because the coordination environment of oxygen is significantly disturbed on material surfaces during material preparation. As mentioned before, activated carbon is made from a raw material generally through a two stage process: carbonization and activation. Carbonization removes oxygen from the precursor material [34], at least from the outer shells of the resulting char particles. The calcined material is then activated by adsorbing

water or oxygen molecules onto material surfaces to form various oxygen-containing functional groups. As shown in Figure 3B, the oxygen spectra indeed show a significant difference between the two types of activated carbon materials. The peaks of oxygen spectra for type I materials systematically shift to lower energies as compared to type II materials (Figure 3), indicating that type I materials possess more C=O and fewer C-O bonds in their surface functional groups than type II materials [31, 35, 36], which is consistent with our acid-base titration results showing the presence of a significant fraction of carboxylic groups in type I materials (see Section 3.3).

### 3.3 Surface acidity of activated carbon

The pH titration results for materials INSUL, S-51HF, HYDRO-4000 and 12X20DC are shown in Figure 4A. The two types of activated carbon materials exhibit very different titration behaviors, with the type II materials (HYDRO-4000 and 12X20DC) having a much less buffering capacity around pH 6. We have also conducted titrations with different ionic strengths using NaCl as a background electrolyte. We have found that the surface chemistry of type I materials is more or less insensitive to ionic strength changes as long as the concentration of NaCl is below 0.01 M, indicating that the surface chemistry of these material is controlled by inner sphere chemical complexation rather than by electrostatic interactions. The titration results also indicate that type II materials have a relatively higher affinity for adsorption of chlorite anions.

The surface charge density ( $\sigma_0$ ) of each activated carbon is defined as [37]:

$$\sigma_0 = \frac{(c_A - c_B + [OH^-] - [H^+])F}{Sa} \quad (2)$$

where  $C_A$  and  $C_B$  are the concentrations of acid and base needed to reach a point on the titration curve (in M);  $[H^+]$  and  $[OH^-]$  are the concentrations of  $H^+$  and  $OH^-$  (in M);  $F$  is the Faraday constant (96,490 Coulomb/mol);  $S$  is the specific surface area (in  $m^2/g$ ), and  $a$  is the concentration of activated carbon (in g/l). The surface charge density as a function of solution pH for each activated carbon is depicted in Figure 4B. The difference in surface charge distribution between the two types of materials is evident. Within the pH range of 4 - 10, the surface charge densities on type I materials are much

higher than those on type II materials. The zero point of charge of is found to be about 6.5 for type I materials and 9.0 for type II materials.

The heterogeneity of surface functional groups of activated carbon can be characterized by the distribution of acidity constants or proton binding affinities. With the assumption that proton uptake on a single of population binding sites follows a Langmuir isotherm, the overall degree of protonation of activated carbon surfaces,  $Q$ , can be related to the binding site distribution,  $f(pK)$ , and the acidity constants,  $pK$ , by the following equation [38]:

$$Q = \int_{pK_{\min}}^{pK_{\max}} \frac{f(pK)}{1 + 10^{-pK+pH}} d(pK), \quad (3)$$

where  $Q$  can be calculated from the titration curves in Figure 4A. The distribution of acidity constants can be calculated by deconvolution of Equation (3) using a so-called condensation approximation [38]:

$$f(pK) \approx -\frac{dQ}{dpH}. \quad (4)$$

The derivative in Equation (4) is calculated using a five-point smoothing window. The calculated distribution of acidity constants for each material is shown in Figure 5.

The difference in the distribution of surface acidity constants between the two types of activated carbon materials is evident (Figure 5). In type I materials, four  $f(pK)$  peaks are identified at the  $pK$  values about 4.0, 5.5, 8.5, and 10.0 (Figure 5 A and B).

Functional groups on activated carbon can be categorized into two general groups: carboxylic groups and phenolic groups [31, 39-42]. Note that polymerization of acids tends to generate molecules with weaker acidity (i.e. a high  $pK$  value) [43]. For example, only about 60% of carboxylic groups in natural organic matters are deprotonated at pH 8.0 [44]. We thus assign the first three peaks to carboxylic groups and the last peak to phenolic groups (Figure 5). The carboxylic groups can be further divided into subgroups A, B, and C in the order of increasing acidity. It is interesting to note that type II materials only have two peaks in  $f(pK)$ , corresponding to carboxylic subgroup C and phenolic groups (Figure 5C and D), and carboxylic subgroups A and B are conspicuously

missing. This difference in the distribution of surface functional groups is expected to be the major cause for the distinct behaviors of two types of activated carbons in uptake of  $\text{TcO}_4^-$ . Therefore, carboxylic subgroups A and B must have higher Tc sorption capabilities than other functional groups, for the reason given below.

### 3.4 Sorption mechanism and its implications to material engineering

On each carboxylic group  $\text{R}-\overset{\text{OH}}{\text{C}}=\text{O}$ , there exist two potential binding sites for pertechnetate sorption:  $\text{R}-\text{C}-\text{OH}$  and  $\text{R}-\text{C}=\text{O}$ , where R represents aromatic rings. At the  $\text{R}-\text{C}-\text{OH}$  site,  $\text{TcO}_4^-$  is adsorbed by displacing the hydroxyl group in the acid,  $\text{R}-\text{C}-\text{OH} + \text{TcO}_4^- \rightarrow \text{R}-\text{C}-\text{OTcO}_3^- + \text{OH}^-$ , with one  $\text{TcO}_4^-$  adsorbed and one  $\text{OH}^-$  released. The sorption of  $\text{TcO}_4^-$  to the  $\text{R}-\text{C}=\text{O}$  site is probably through hydrogen bonding or electrostatic attraction:  $\text{R}-\text{C}=\text{O} \cdots \text{H}^+ + \text{TcO}_4^- \rightarrow \text{R}-\text{C}=\text{O} \cdots \text{H}^+ \cdots \text{OTcO}_3^-$ , with no net consumption or release of  $\text{H}^+$ . It is important to note that the bonds of C-OH and C=O in a carboxylic acid are conjugated and switch between them constantly. Thus,  $\text{TcO}_4^-$  attaches to each site with an equal probability. As a result, on average, the adsorption of one  $\text{TcO}_4^-$  onto a carboxylic group releases 0.5  $\text{OH}^-$ , which is surprisingly consistent with the slope of the sorption line for type I materials Figure 1. Because of the direct involvement of C- $\text{TcO}_4^-$  bonding, carboxylic subgroups A and B, and therefore the type I materials, have high Tc sorption capabilities.

$\text{TcO}_4^-$  seems not able to displace hydroxyl groups in both phenolic groups and carboxylic subgroup C, because otherwise a strong pH dependence of sorption line for type II materials would be observed in Figure 1. Phenolic groups are likely to remain protonated for  $\text{pH} < 10$ . It is thus possible for  $\text{TcO}_4^-$  to attach to these functional groups through either hydrogen bonding or electrostatic attraction:  $\text{R}-\text{OH}_2^+ + \text{TcO}_4^- \rightarrow \text{R}-\text{OH}^+ \cdots \text{OTcO}_3^-$ . Since carboxylic subgroup C is expected to be completely deprotonated above pH 4, the contribution of this functional group to  $\text{TcO}_4^-$  sorption is probably negligible. The hydrogen bonding, which is equivalent to an outer sphere complexation, is expected to be much weaker than the direct C- $\text{OTcO}_3^-$  bonding in carboxylic subgroups

A and B. As a result, type II materials, which are dominated by phenolic groups, have much lower sorption capabilities (Figure 1).

The Tc sorption on activated carbon was suspected to involve reduction of Tc(VII) to Tc(IV), based on the observed high  $K_d$  values [25]. Our data presented above, however, do not support this hypothesis. If the Tc uptake by activated carbon were controlled by reduction, the measured  $K_d$  value would increase with pH, because the solubility of the reduced Tc solid phase,  $TcO_2 \cdot nH_2O$ , decreases with increasing pH, and also because the sorption of dissolved species,  $Tc^{4+}$ , increases with pH. This is apparently contradictory to our observations (Figure 1). In addition, the hypothesis seems not compatible with the manufacturing process of activated carbon. To form oxygen-containing surface functional groups, a calcined carbonaceous material is activated (i.e., oxidized) at elevated temperatures in the presence of air or water steams. If the Tc uptake by activated carbon were controlled by reduction, such activation process would tend to decrease the sorption capability of the material. On the contrary, activated carbon has much higher sorption capabilities than raw or un-activated carbonaceous materials [24].

The sorption mechanism proposed above has important implications to material selection and engineering. Our work shows that a high-performance adsorbent for removing pertechnetate can be developed by enhancing the formation of carboxylic subgroups A and B on activated carbon surface during activation. Activated carbon engineered as such may have a  $K_d$  value as high as  $10^6$  mL/g. With such high sorption capability and also due to its large-scale availability, activated carbon could be an ideal barrier material for radioactive waste isolation. Since the Tc sorption on activated carbon does not rely on reduction of Tc(VII) to Tc(IV), such barrier material is expected to remain effective in an oxidizing environment. Evidences also indicate that activated carbon will be durable over a long-time period under anticipated geologic repository conditions. First of all, activated carbon is made and activated at elevated temperatures up to  $1000^\circ C$  [7, 8, 41], and it is unlikely that the heat from radiation decay will degrade the performance of this material as an adsorbent. Second, as a matter of fact, aging or heating the material in the air at a moderate temperature tends to add more oxygen-

containing functional groups to material surfaces [30, 35], which may even enhance the sorption capability. It has been reported that carboxylic groups are stable at least at temperature 300 °C [35]. Ion selectivity might be a potential issue that needs to be further tested for the applications in waste isolation. Nevertheless, the existing data suggest that activated carbon is able to selectively remove  $\text{TcO}_4^-$  from groundwater and background solutions of 0.01 M  $\text{CaCl}_2$  and  $\text{Na}_2\text{SO}_4$  [1].

#### **4. Conclusion**

Six commercial activated carbon materials have been tested for their capabilities for sorption of pertechnetate ( $\text{TcO}_4^-$ ). The results show that the materials can be grouped into two general types: Type I materials have high sorption capabilities with the distribution coefficients ( $K_d$ ) varying from  $9.5 \times 10^5$  to  $3.2 \times 10^3$  mL/g as the pH changes from 4.5 to 9.5., whereas type II materials have relatively low sorption capabilities with  $K_d$  remaining more or less constant ( $1.1 \times 10^3$  -  $1.8 \times 10^3$  mL/g) over a similar pH range. Such a striking difference in sorption behavior between the two types of materials is attributed to the different distribution of functional groups on material surfaces. Both FTIR and XPEEM analyses indicate that the predominant surface groups include carboxylic acids and phenolic hydroxyl. Acid-base titration analyses suggest that the carboxylic group can be further divided into three subgroups A, B, and C in the order of increasing acidity. The presence of a large fraction of carboxylic subgroups A and B is found to be responsible for the high sorption capabilities observed for type I materials. Whereas, the low  $K_d$  values measured for type II materials are due to the exclusive presence of phenolic hydroxyl and carboxylic subgroup C. The work reported here will help to select or engineer an effective pertechnetate adsorbent for radioactive waste disposal.

#### **Acknowledgments**

This work was performed at Sandia National Laboratories (SNL), which is a multiprogram laboratory operated by Sandia Corporation, a Lockheed-Martin Company, for the DOE under contract DE-AC04-94AL8500. The work was supported by DOE Office of Civilian Radioactive Waste Management (OCRWM) through its Science and

Technology Program and the Graduate School of University of Wisconsin - Madison. Authors would like to thank Bill Naylor of NORIT Americas Inc. for generously providing activated materials and the related information.

## References

- [1] B. Gu, K. E. Dowlen, L. Liang, J. L. Clausen, *Separation Technology* 6 (1996) 123.
- [2] J. Wengle, Office of Science and Technology and International Annual Report 2005, U.S. Department of Energy Office of Civilian Radioactive Waste Management, Washington, D. C, 2005.
- [3] K. H. Lieser, Ch. Bauscher, *Radiochim. Acta* 42 (1987) 205.
- [4] K. Wildung, M. Mcfadden, T. R. Garland, *J. Environ. Qual.* 8 (1979) 156.
- [5] Y. Wang, C. Bryan, H. Gao, P. I. Pohl, C. J. Brinker, K. Yu, H. Xu, Y. Yang, P. S. Braterman, Z. Xu, *Potential Applications of Nanostructured Materials in Nuclear Waste Management*, Sandia National Laboratories, Albuquerque, New Mexico, 2003.
- [6] Y. Wang, H. Gao, *J. Colloid and Interface Sci.* (2006) (in press).
- [7] J. S. Mattson, H. B. Mark, *Activated Carbon: Surface Chemistry and Adsorption from Solution*, Marcel Dekker, New York, 1971.
- [8] H. Jankowska, A. Swiatkowski, J. Choma, *Activated Carbon*, Ellis Horwood, Chichester, UK, 1991.
- [9] M. O. Corapcioglu, C. P. Huang, *Wat. Res.* 21 (1987) 1031.
- [10] Y. F. Jia, K. M. Thomas, *Langmuir* 16 (2000) 1114.
- [11] B. Xiao, K. M. Thomas, *Langmuir* 21 (2005) 3892.
- [12] M. Siddiqui, W. Zhai, G. Amy, C. Mysore, *Wat. Res.* 30 (1996) 1651.
- [13] M. L. Bao, O. Griffini, D. Santianni, K. Barbieri, D. Burrini, F. Pantani, *Wat. Res.* 33 (1999) 2959.
- [14] B. Daus, R. Wennrich, H. Weiss, *Wat. Res.* 38 (2004) 2948.
- [15] M. Sánchez-Polo, J. Rivera-Utrilla, E. Salhi, U. von Gunten, *J. Colloid and Interface Sci.* (2006) (in press).
- [16] M. Streat, J. W. Patrick, M. J. Camporro Perez, *Wat. Res.* 29 (1995) 467.
- [17] M. P. Cal, M. J. Rood, S. M. Larson, *Gas. Sep. Purif.* 10 (1996) 117.

- [18] C. Brasquet, P. Le Cloirec, *Langmuir* 15 (1999) 5906.
- [19] F. Haghseresht, S. Nouri, J. J. Finnerty, G. Q. Lu, *J. Phys. Chem.* 106 (2002) 10935.
- [20] H. E. van Dam, H. van Bekkum, *J. Catalysis* 131 (1991) 335.
- [21] L. Eliad, G. Salitra, A. Soffer, D. Aurbach, *J. Phys. Chem.* 105 (2001) 6880.
- [22] A. Lewandowski, M. Galiński, *J. Phys. Chem. Solids* 65 (2004) 281.
- [23] F. Béguin, K. Hierzek, M. Friebe, A. Jankowska, J. Machnikowski, K. Jurewicz, E. Frackowiak, *Electrochimica Acta* 51 (2006) 2161.
- [24] K. Ito, A. Yachidate, *Carbon* 30 (1992) 767.
- [25] E. Holm, T. Gäfvert, P. Lindahl, P. Roos, *Applied Radiation and Isotopes* 53 (2000) 153.
- [26] S. J. Gregg, K. S. W. Sing, *Adsorption Surface Area and Porosity*, 2<sup>nd</sup> ed., Academic Press, London, 1982.
- [27] G. M. K. Abotsi, A. W. Scaroni, *Carbon* 28 (1990) 79.
- [28] Y. F. Jia, B. Xiao, K. M. Thomas, *Langmuir* 18 (2002) 470.
- [29] V. Boonamnuayvitaya, S. Sae-ung, W. Tanthapanichakoon, *Sep. Purif. Technol.* 42 (2005) 159.
- [30] M. O. Corapcioglu, C. P. Huang, *Carbon* 25 (1987) 569.
- [31] S. Biniak, G. Szymański, J. Siedlewski, A. Świątkowski, *Carbon* 35 (1997) 1799.
- [32] J. G. Chen, *Surface Science Reports* 30 (1997) 1.
- [33] J. Stohr, *NEXAFS Spectroscopy*, Springer Series in Surface Science, Vol. 25, Springer, New York, 1992.
- [34] P. Chingombe, B. Saha, R. J. Wakeman, *Carbon* 43 (2005) 3132.
- [35] G. de la Puente, J. J. Pis, J. A. Menéndez, P. Grange, *J. Analytical and Applied Pyrolysis* 43 (1997) 125.
- [36] S.J. Park, Y.-S. Jang, *J. Colloid and Interface Sci.* 249 (2002) 458.
- [37] Y. Wang, C. Bryan, H. Xu, P. Pohl, Y. Yang, C. J. Brinker, *J. Colloid and Interface Sci.* 254 (2002) 23.
- [38] C. Contescu, J. Jagiello, J. A. Schwarz, *Langmuir* 9 (1993) 1754.
- [39] T. J. Bandosz, J. Jagiello, C. Contescu, J. Schwarz, *Carbon* 31 (1993) 1193.
- [40] I. I. Salame, T. J. Bandosz, *Langmuir* 15 (1999) 587.
- [41] V. Strelko Jr., D. J. Malik, M. Streat, *Carbon* 40 (2002) 95.

- [42] A. M. Puziy, O. I. Poddubnaya, A. Martínez-Alonso, F. Suárez-García, J. M. D. Tascón, *Carbon* 41 (2003) 1181-1191.
- [43] H. Morawetz, *Macromolecules in Solution*, 2<sup>nd</sup> ed., John Wiley, New York, 1975.
- [44] M. Edwards, M. M. Benjamin, J. N. Ryan, *Colloids and Surfaces A: Physicochemical and Engineering Aspects* 107 (1996) 297.
- [45] P. E. Fanning, M. A. Vannice, *Carbon* 31 (1993) 721.
- [46] V. M. Gun'ko, R. Leboda, J. Skubiszewska-Zięba, B. Charmas, P. Oleszczuk, *Carbon* 43 (2005) 1143.
- [47] D. J. Kim, H. I. Lee, J. E. Yie, S.-J. Kim, J. M. Kim, *Carbon* 43 (2005) 1868.
- [48] V. Gómez-Serrano, M. Acedo-Ramos, A. J. López-Peinado, C. Valenzuela-Calahorra, *Fuel* 73 (1994) 387.

**Figure captions:**

Figure 1. Distribution coefficients of Tc between activated carbon materials and aqueous solutions as a function of pH.

Figure 2. Fourier transformation infrared (FTIR) spectroscopic analyses of four representative activated carbon materials.

Figure 3. X-ray photoelectron emission spectromicroscopic analyses of four representative activated carbon materials. A – carbon spectra, B – oxygen spectra.

Figure 4. Acid-base titration curves and surface charge densities for four representative activated carbon materials.

Figure 5. Distributions of acidity constants for four representative activated carbon materials.

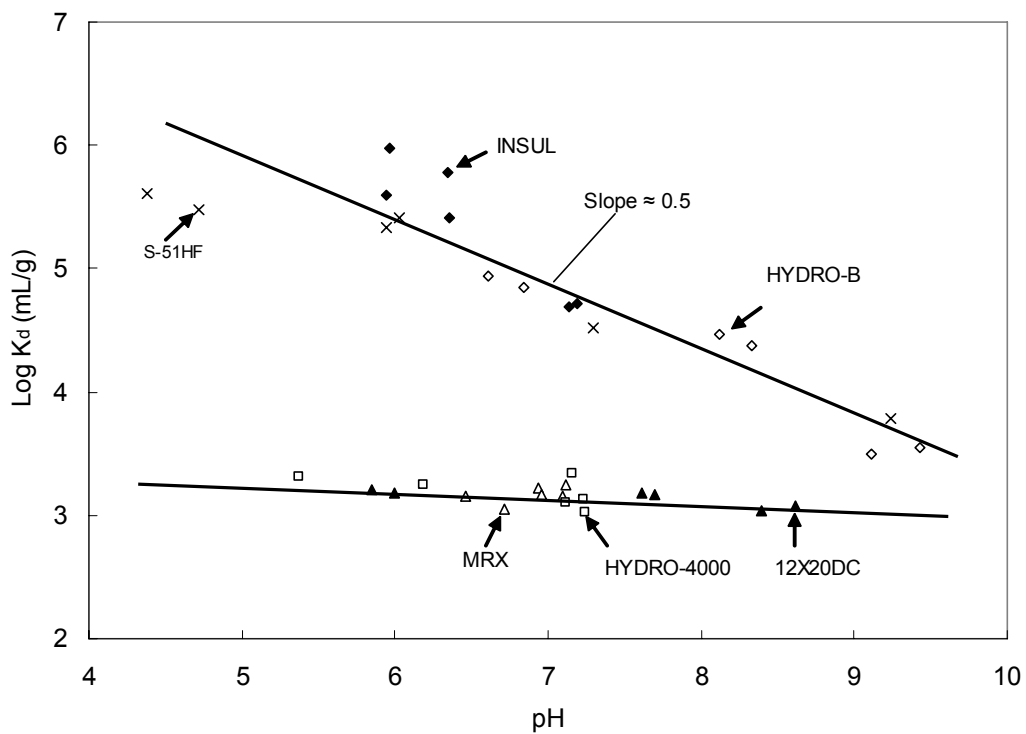


Figure 1

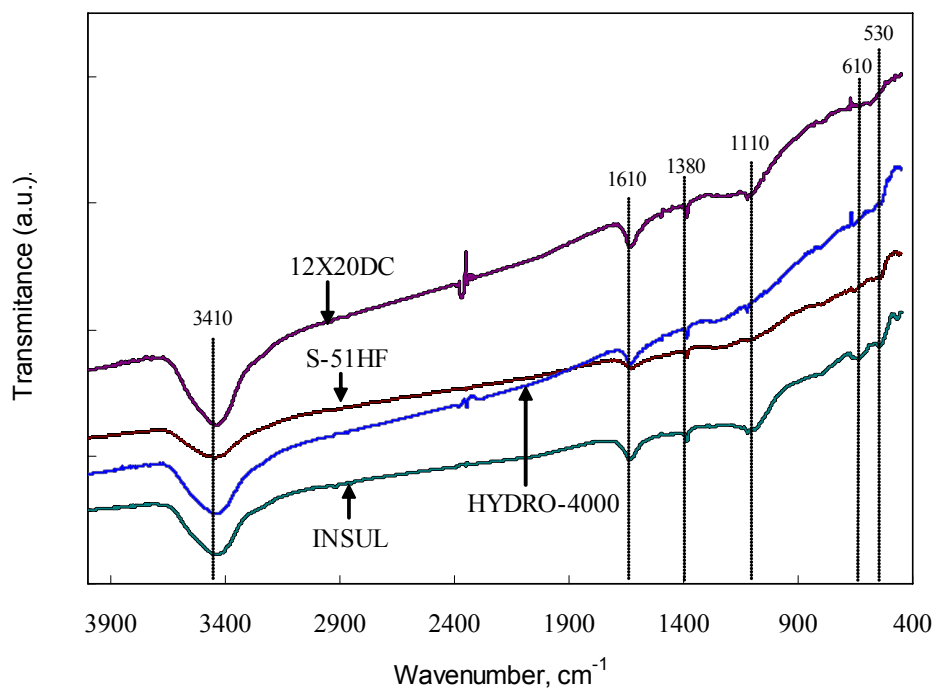


Figure 2

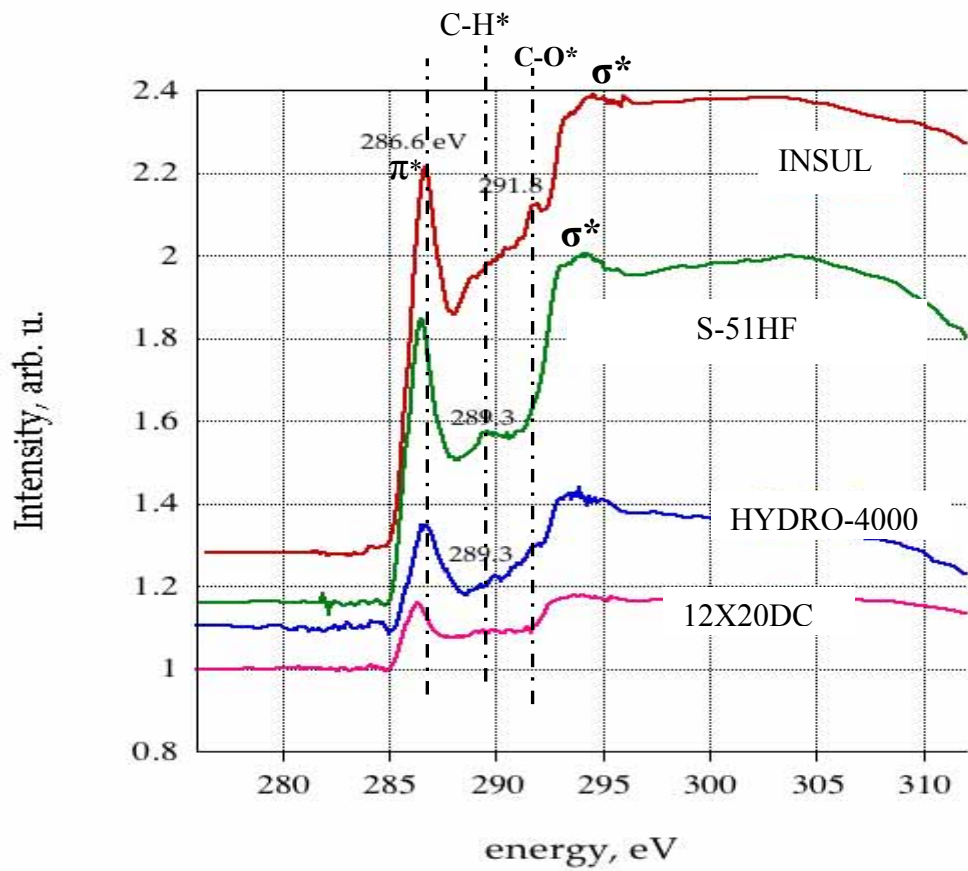


Figure 3A

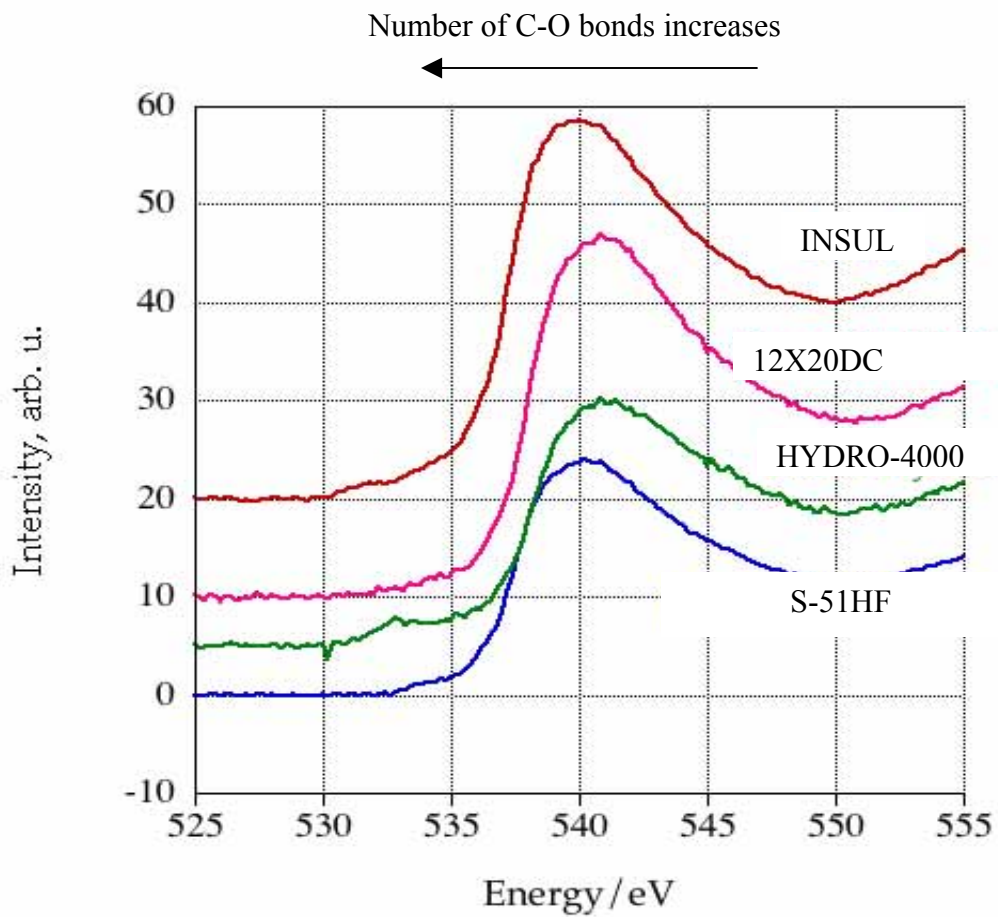


Figure 3B

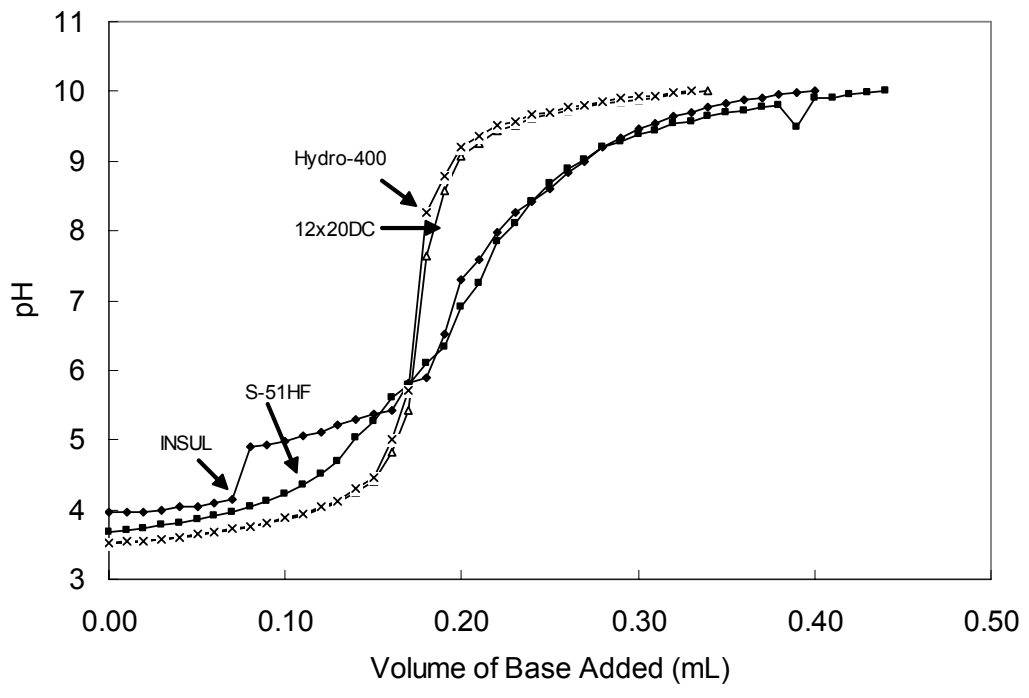


Figure 4A

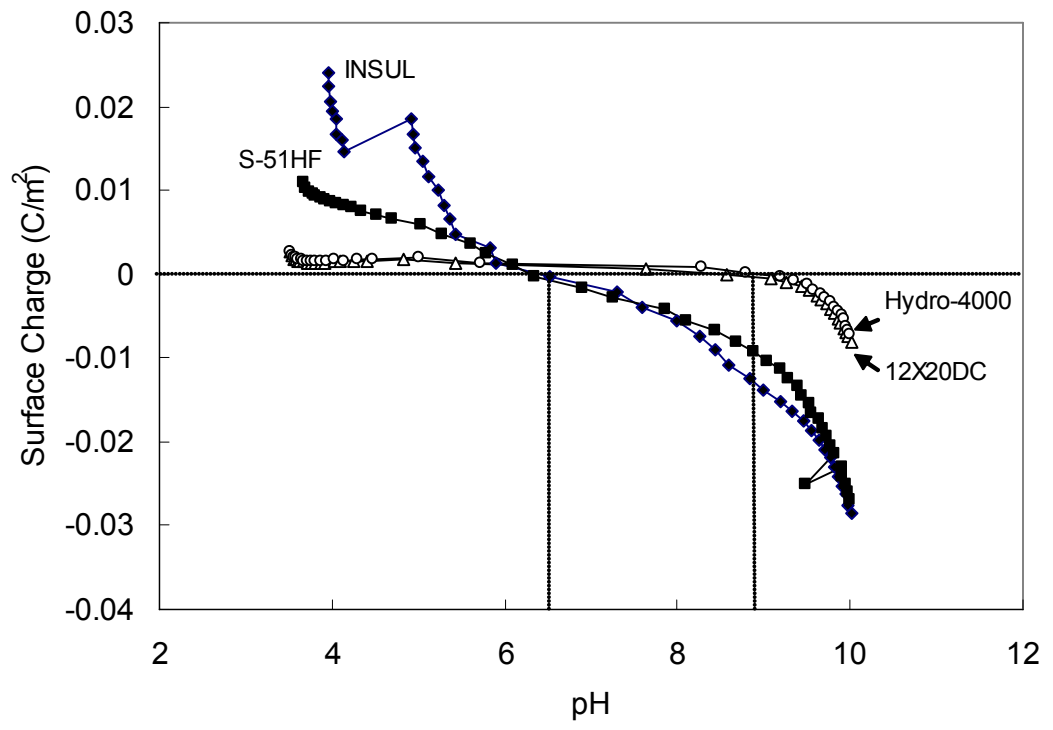


Figure 4B

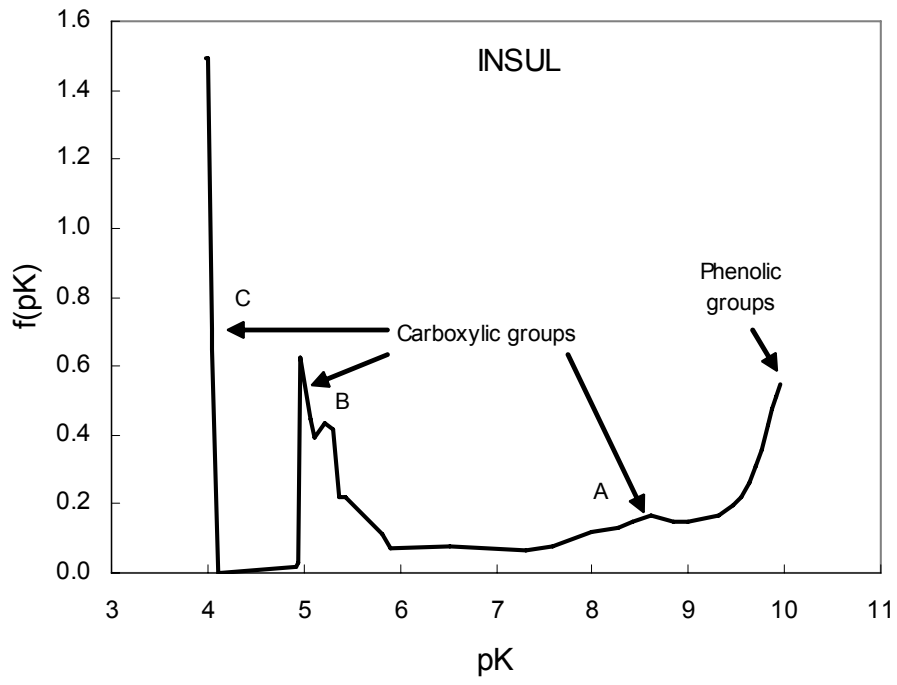


Figure 5A

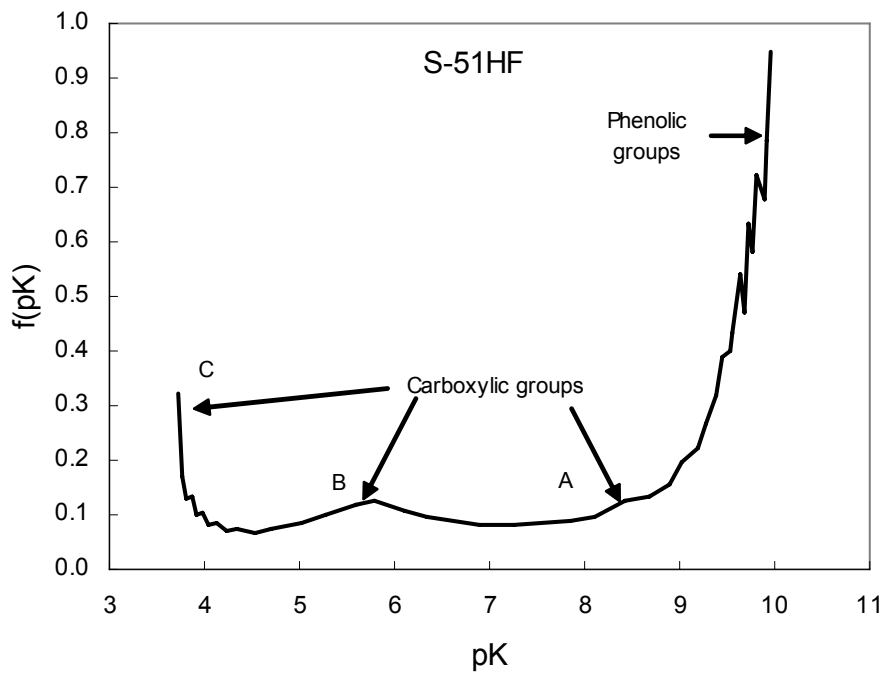


Figure 5B

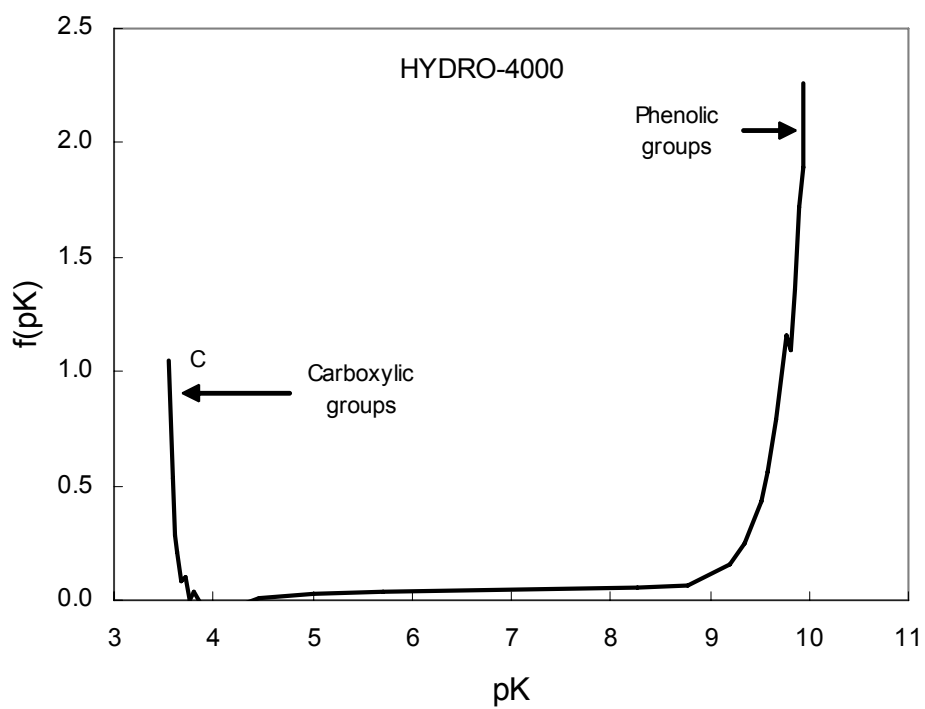


Figure 5C

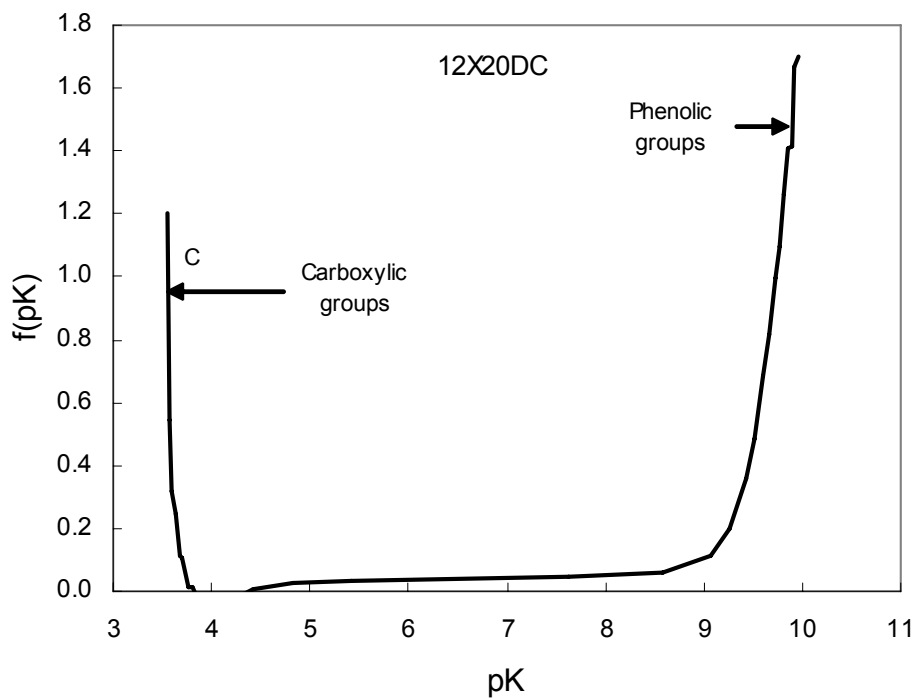


Figure 5D

**Table 1.** Surface area and pore size of activated carbon materials

Activated carbon	Surface area m <sup>2</sup> /g	Average pore size nm	Total volume cc/g
INSUL	489	4.6	0.56
HYDRO-B	468	4.3	0.50
HYDRO-4000	750	4.1	0.76
12X20DC	538	4.9	0.66
MRX	557	5.4	0.76
S-51HF	640	4.8	0.77

**Table 2.** FTIR spectrum band assignments

Band number (cm <sup>-1</sup> )	Assignment	Reference
3411	O-H stretching vibration in surface hydroxylic, carboxylic, and phenolic groups	[10, 29, 45]
1613	C=C stretching vibration in carboxylic groups	[29, 45, 46]
1381	C-H deformation vibration in alkane	[29]
1111	C-O stretching vibration in phenolic and carboxylic groups	[11, 29, 45, 46]
<700	C-H vibration	[47, 48]